Journal of Power Sources 180 (2008) 830–835

Contents lists available at ScienceDirect

Journal of Power Sources

journal homepage: www.elsevier.com/locate/jpowsour

Short communication

Influence of temperature on the electrochemical characteristics of $MmNi_{3.03}Si_{0.85}Co_{0.60}Mn_{0.31}Al_{0.08}$ hydrogen storage alloys

M. Raju [a], M.V. Ananth [a,*], L. Vijayaraghavan [b]

[a] Nickel-Metal Hydride Battery Section, Electrochemical Power Systems Division, Central Electrochemical Research Institute, Karaikudi 630006, India
[b] Department of Mechanical Engineering, Indian Institute of Technology Madras, Chennai 600036, India

ARTICLE INFO

Article history:
Received 24 October 2007
Received in revised form 19 December 2007
Accepted 6 February 2008
Available online 29 February 2008

Keywords:
Metal hydride electrode
Charge/discharge performance
Electrochemical
pressure–composition–temperature
isotherms
Impedance spectrum
Thermodynamic parameters
Hydrogen storage

ABSTRACT

The heat of hydride formation is a crucial parameter in characterizing a hydrogen storage alloy for battery applications. Novel AB_5-type, non-stoichiometric, lanthanum-rich $MmNi_{3.03}Si_{0.85}Co_{0.60}Mn_{0.31}Al_{0.08}$ (Mm: Misch metal) hydrogen storage metal hydride alloy electrodes are prepared. Electrochemical hydrogen absorption/desorption and electrochemical impedance measurements are carried out at various temperatures in conjunction with sintered nickel hydroxide positive electrodes. The specific capacity of the prepared metal hydride electrodes decreases from 283 mAh g^{-1} at 303 K to 213 mAh g^{-1} at 328 K. Electrochemical pressure–composition–temperature (PCT) isotherms are constructed from galvanostatic discharge curves and the change in enthalpy (ΔH_e°) and the change of entropy (ΔS_e°) of the metal hydride alloy electrodes are evaluated as −41.74 kJ mol^{-1} and 146.28 J mol^{-1} K^{-1}, respectively. Kinetic parameters are obtained by fitting the electrochemical impedance spectrum performed at different temperatures. The charge-transfer resistance decreases with temperature, whereas exchange current density and diffusion coefficient parameters increase with temperature. It is concluded that the deterioration in capacity is due to enhanced surface activity at higher temperatures.

1. Introduction

Nickel–metal hydride (Ni–MH) batteries have been the focus of attention since 1990 due to their inherent advantages of high specific energy, high-rate capability, and freedom from toxic materials. They find application in computers, cameras, camcorders, emergency lighting units, telecommunication systems, and hybrid electric vehicles. They are also serious contenders for electric vehicles. The performance of the system relies on the electrochemical activity of the metal hydride alloy negative electrode, which supplants the toxic cadmium electrode in the conventional nickel–cadmuim (Ni–Cd) cell. The negative electrode can be prepared from a variety of intermetallic compounds, whose hydrogen absorption/desorption characteristics decide the performance of the Ni–MH cell. Hong [1] reported a semi-empirical method for the preparation of hydrogen-absorbing metal hydride alloys based on thermodynamic and electrochemical studies.

Metal hydrides for battery applications are characterized in terms of their hydrogen storage capacity at moderate hydride stability and approximately constant equilibrium pressure during hydride phase transformation. Data on these properties can be obtained from pressure–composition–temperature (PCT) isotherms, which describe the dependence of the hydrogen equilibrium pressure on the amount of hydrogen absorbed or incorporated into the hydrogen storage material at various temperatures. Thermodynamic properties such as the change in enthalpy (ΔH) and the change in entropy (ΔS) can be calculated from PCT isotherms [2]. The PCT isotherms can also be used to identify different phases in metal hydride alloys. Hydrogen concentration at various stages such as in the α-phase, during transition of α-phase to β-phase, and in the β-phase in equilibrium with the α-phase can also be obtained from PCT isotherms [3]. PCT diagrams can be constructed for metal hydride alloys in two ways, namely, a gas–solid PCT isotherm and an electrochemical PCT isotherm. In general, the plateau pressure for the metal hydride electrode at room temperature is lower than 1 atm, which calls for specially designed high-vacuum equipment as well as a long period for attaining hydrogen equilibrium pressure. If the plateau pressure is much lower than 1 atm, then it is impossible to attain the equilibrium pressure [4]. The electrochemical approach to construct PCT isotherms, therefore, is a simple and convenient alternative procedure. Despite the importance of the heat of hydride formation of metal hydrides for battery applications, sufficient studies have not appeared in the literature, especially by electrochemical methods.

Hong [1] reported that the heat of hydride formation for titanium/zirconium-based metal hydrides was in the range of

* Corresponding author. Tel.: +91 4565 227555; fax: +91 4565 227713.
E-mail address: mvananth@rediffmail.com (M.V. Ananth).

0378-7753/$ – see front matter © 2008 Elsevier B.V. All rights reserved.
doi:10.1016/j.jpowsour.2008.02.061

−24.83 to −29.68 kJ mol^{-1} and those of rare earth metal-based hydrides were −18.56 to −20.11 kJ mol^{-1}. Kleperis et al. [5] and Ovshinsky et al. [6] found that alloys with ΔH values between −25 and −50 kJ mol^{-1} were suitable for battery applications. On the other hand, Hong [7] postulated that the heat of formation of hydrides should be between −15 and −40 kJ mol^{-1}. A value lower than −15 kJ mol^{-1} renders the alloy not sufficiently stable for charging at room temperature, whereas a ΔH value exceeding −50 kJ mol^{-1} should render it too stable for room temperature discharge. In practice, ΔH is an index of the thermochemical stability of metal hydride electrodes. A high ΔH value would signify a high degree of stability of the hydride and low dissociation pressures, which means that a high temperature is required to decompose the alloy to release the hydrogen. On the contrary, an alloy with a low ΔH value would have characteristics opposite to those discussed above [8].

Bouten and Miedema [9], Oesterreicher [10], Griessen [11] and Shilov et al. [12] proposed models to determine the heat of formation of hydrides using different atomic parameters. Shuang et al. [13] constructed semi-empirical model for the heat of formation of hydrides and hydrogen concentration in $LaNi_{5-x}M_x$ alloys. They used several atomic parameters such as atomic size, electronegativity, electron density and charge–radii ratio to construct the model via a stepwise regression method. The model has been used only for the ternary $LaNi_5$-based alloy hydrides, however, and not for multicomponent alloys and non-stoichiometric AB_2 alloys with different substitutions at the A and B sites. Recently, Mani et al. [14–17] and Kandavel et al. [18] systematically investigated the hydrogen storage properties of Zr-based C14 AB_2-type alloys, Mm-based AB_5-type alloys and Ti-substituted AB_2-type alloys in order to assess the suitability of these materials for hydrogen storage devices. Since refined calculations of the heat of formation of hydrides require considerable computing efforts, only semi-empirical models have been investigated. It has been found that the amount of hydrogen absorbed in $LaNi_{5-x}M_x$ alloys is controlled by electronegativity differences, atomic size, electron concentration and charge–radii ratio [13].

Ni–MH batteries give the best performance between 20 and 40 °C. The temperature at which the battery is discharged has a pronounced effect on its capacity and voltage characteristics. This is because discharge capacity and cell voltage are strongly dependent on the operating temperature. The rate of hydrogen diffusion within the bulk of the electrode and the processes occurring at the electrode–electrolyte interface are dependent upon temperature, and hence the present investigation becomes important. Previous efforts in this direction were mostly aimed at studies of kinetic parameters as a function of the state-of-charge of the electrode at ambient temperatures [19–21]. Only a few have concentrated on the temperature dependence of the hydrogen diffusion coefficient in metal hydride electrodes. This communication describes the preparation of a novel La-rich metal hydride electrode and its performance degradation at elevated temperatures. Generally, electrochemical kinetics can be described by electrode resistance, exchange current density and diffusion coefficient. The effect of temperature on these parameters as applied to an $MmNi_{3.03}Si_{0.85}Co_{0.60}Mn_{0.31}Al_{0.08}$ hydrogen storage alloy are reported.

2. Experimental

Non-stoichiometric, lanthanum-rich, AB_5-type rare earth metal-based hydride alloy powder of $MmNi_{3.03}Si_{0.85}Co_{0.60}Mn_{0.31}Al_{0.08}$ was used to prepare the negative electrode of the nickel–metal hydride cell. The La:Ce ratio in Mm was 11.65. The alloy was prepared by button arc melting followed by necessary treatment at the Defence Metallurgical Research Laboratory (DMRL), Hyderabad, India. The purity of the constituent metals (La, Ce, Ni) was at least 99.9%. In order to ensure homogeneity, ingots were turned over and melted twice. The ingots were mechanically pulverized into fine powders of sieve size less than 75 μm. The composition of the product was determined by X-ray fluorescence spectroscopy (Horiba XRF Analyzer, model XGT-2700).

Test electrodes for galvanostatic charge/discharge experiments were made from 1.00 g of the alloy and had a geometrical area of 3 cm × 2 cm. Electrodes for impedance measurements were made from 0.170 g of the alloy and had a geometrical area of 1 cm × 1 cm. A slurry of the alloy powder with appropriate amounts of conducting carbon powder and polytetrafluoroethylene binder was applied to both sides of a nickel foam substrate, dried and compacted under 75 MPa pressure, and finally heat-treated at 408 K for 1 h.

The test cell was comprised of the alloy as the working electrode, a sintered $Ni(OH)_2$ electrode (of higher capacity than the working electrode) as the counter electrode, and Hg|HgO in 6 M KOH as the reference electrode. Galvanostatic charge/discharge cycling was carried out at a current density of 60 mA g^{-1} by means of a Bitrode LCN life cycle tester. Charging was undertaken for 7 h and discharging was continued until the potential of the alloy electrode reached −0.7 V with respect to the reference electrode. Up to 25 charge–discharge cycles were run at 303 K. Subsequently, cycling studies were carried out at 308, 318 and 328 K. Electrochemical impedance experiments were performed with an Auotolab 30 potentiostat/galvanostat between 100 kHz and 5 mHz at a signal amplitude of 5 mV at 100% state-of-charge. Before each measurement, sufficient time was allowed for the system to reach equilibrium conditions.

3. Results and discussion

Metal hydride alloy electrodes generally require more than 15 cycles to complete the activation process and to reach their maximum capacity. The variation of capacity of the $MmNi_{3.03}Si_{0.85}Co_{0.60}Mn_{0.31}Al_{0.08}$ alloy electrode as a function of cycle number over 100 cycles at C/5 rate and at 303K is shown in Fig. 1. From an initial capacity of 111 mAh g^{-1}, the capacity reaches 258 mAh g^{-1} in the fourth cycle. Thereafter, the capacity stabilizes at around 275 mAh g^{-1}. The maximum capacity obtained was 283 mAh g^{-1}. Beyond 40 cycles, there is only a marginal decrease in capacity.

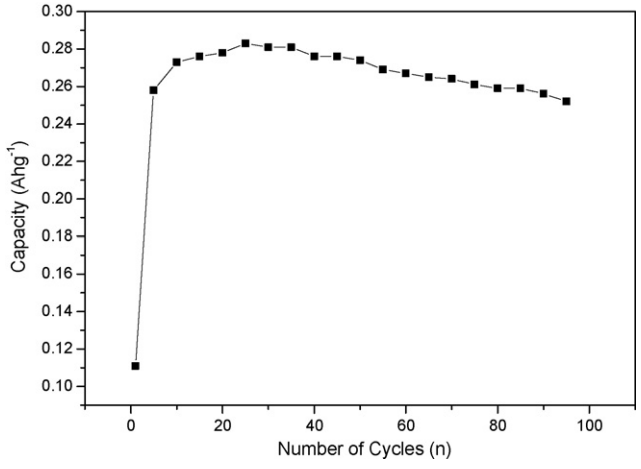

Fig. 1. Cycle-life performance of $MmNi_{3.03}Si_{0.85}Co_{0.60}Mn_{0.31}Al_{0.08}$ electrode at 303 K.

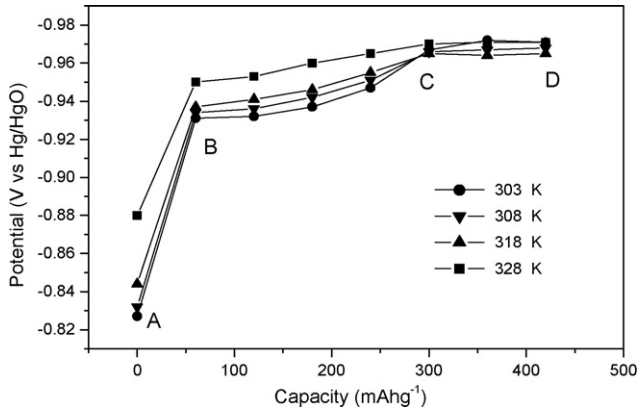

Fig. 2. Charging performance of $MmNi_{3.03}Si_{0.85}Co_{0.60}Mn_{0.31}Al_{0.08}$ electrode at various temperatures.

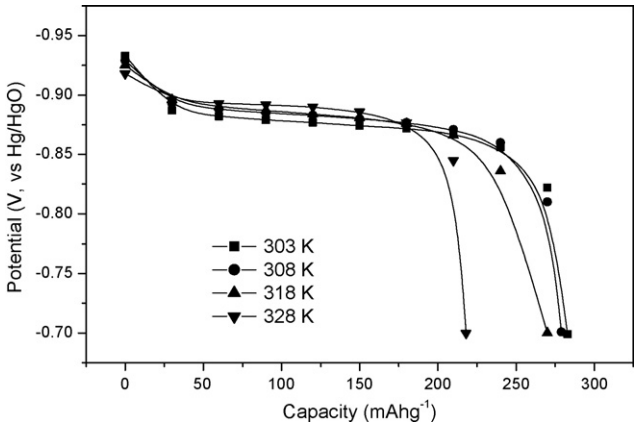

Fig. 3. Discharge performance of $MmNi_{3.03}Si_{0.85}Co_{0.60}Mn_{0.31}Al_{0.08}$ electrode at various temperatures.

The charging curves of the alloy electrode at 303, 308, 318 and 328 K at C/5 rate are shown in Fig. 2. It is seen that the potential profile increases suddenly and reaches almost a plateau region beyond 60 mAh g^{-1}. Furthermore, an increase in the potential plateau is observed with increase in temperature. The charging profiles are evidence for the phase transformations that accompany the charging processes. The region A to B represents the α-phase, in which the hydrogen content is low, $x < 0.1$ H/M (H/M: Hydrogen to metal ratio). The hydrogen absorption–desorption in this single-phase solid solution can be described by the reaction

$$MH_x + \frac{dx}{2}H_2 \Leftrightarrow MH_{x+dx} \quad (1)$$

The region B to C represents the transformation of α-phase to β-phase. The region C to D represents hydrogen evolution. Hydrogen absorption reaches a saturation value at C. Any further charging leads to evolution of hydrogen at the negative electrode. The hydrogen may take part in a recombination reaction with oxygen liberated at the positive electrode. For $0.1 < x < 0.8$ H/M, there is a two-phase domain. Here, the saturated α-phase ($x = \alpha_{max}$) transforms into the β-phase ($x = \beta_{min}$). It corresponds to a plateau pressure, the composition range of which extends as long as the following equilibrium reaction takes place:

$$MH_x(\alpha_{max}) + \frac{y-x}{2}H_2 \Leftrightarrow MH_y(\beta_{min}) \quad (2)$$

A solid–solution, single-phase domain also occurs at $x > 0.8$ H/M, which is the region corresponding to the β-phase. This can be described according to Eq. (1). The discharge performance of the alloy electrode at various temperatures is shown in Fig. 3. Variation in temperature significantly affects the performance of the metal hydride electrode. The performance curve shows that the specific capacity decreases as the temperature is raised. The capacity falls from 283 mAh g^{-1} at 303 K to 213 mAh g^{-1} at 328 K. It is also seen that at the highest temperature studied (328 K), the electrode potential reaches a maximum value and exhibits the highest capacity fade. At elevated temperatures, some amount of hydrogen or oxygen could be liberated and this could adversely affect battery performance, e.g., reduced cycleability, battery swelling, and/or thermal runaway.

The charge–discharge curves under galvanostatic conditions are electrochemical equivalents of the PCT isotherms of the gas–solid phase reaction. In fact, there is a thermodynamic correlation between the equilibrium pressure measured in the gas phase reaction and the electrode potential measured in an electrochemical cell. The potential of the metal hydride electrode in alkaline solution, as measured with respect to a Hg|HgO reference electrode, is converted to the hydrogen equilibrium pressure based on the Nernst equation corresponding to the reversible reaction in Eq. (1):

$$E(V \text{ vs. Hg|HgO}) = -0.932 - 0.0296 \ln P(H_2) \quad (3)$$

where E is the potential of the metal hydride alloy electrode and $P(H_2)$ is the equilibrium hydrogen pressure [3]. A completely charged electrode was discharged at 60 mA g^{-1} for 30 min and allowed to stabilize for 30 min under open-circuit conditions, during which the potential was monitored. After 30 min of open-circuit conditions, it was discharged at the same rate and this cycling was repeated until the potential reached −0.7 V with respect to Hg/HgO. The potential of the metal hydride alloy electrode was converted into the equilibrium pressure of hydrogen using the Nernst equation. An electrochemical PCT isotherm was constructed by plotting the logarithmic equilibrium pressure of hydrogen versus electrochemical absorption capacity according to the van't Hoff relation:

$$\ln\left[\frac{P(H_2)}{P^0}\right] = \frac{\Delta H}{RT} - \frac{\Delta S}{R} \quad (4)$$

where P^0 is the standard pressure, R is gas constant and T is the absolute temperature. The variation of the equilibrium potential under open-circuit conditions after complete charging as a function of temperature is shown in Fig. 4. It can be seen that the equilibrium potential is shifted in a positive direction, which suggests that the hydride alloy is of good quality with low equilibrium hydrogen pressure in the plateau region.

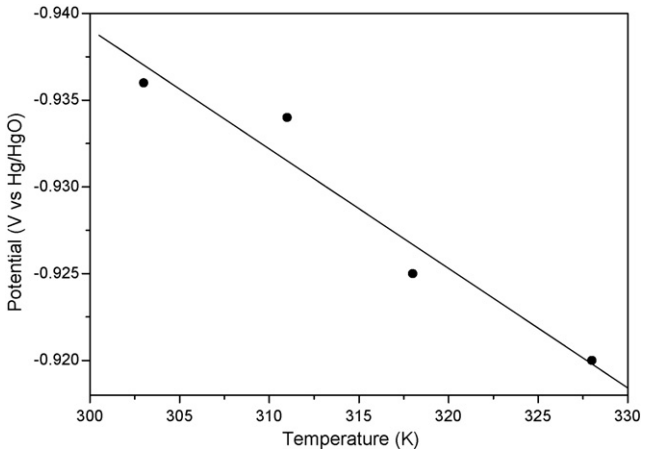

Fig. 4. Relationship between equilibrium potential and temperature.

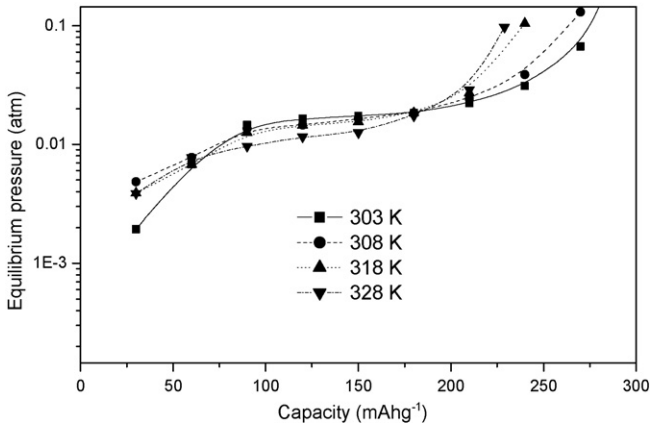

Fig. 5. Electrochemical hydrogen desorption isothermS at various temperatures.

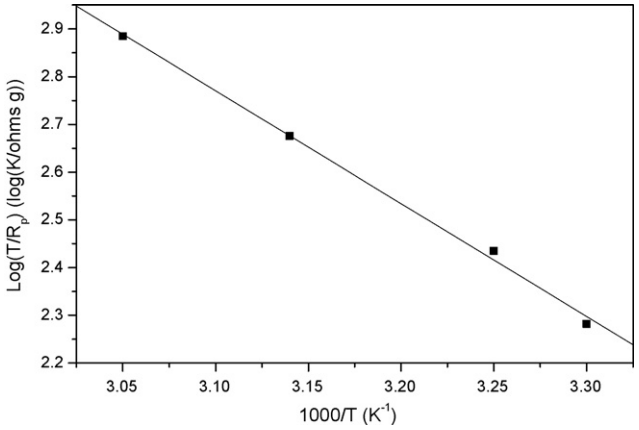

Fig. 7. Relationship between $\log(T/R_p)$ and $1/T$ for prepared metal hydride electrode.

The electrochemical hydrogen desorption isotherms at 303, 308, 318 and 328 K is presented in Fig. 5. The plateau of the hydrogen desorption isotherm decreases with increase in temperature. The van't Hoff plot (logarithm of the equilibrium plateau pressure vs. reciprocal of temperature) for the electrode is given in Fig. 6. The values of ΔH ($-41.74\,\mathrm{kJ\,mol^{-1}}$) and ΔS ($146.28\,\mathrm{J\,mol^{-1}\,K^{-1}}$) were evaluated from the slope and the intercept of van't Hoff plot, respectively. The values are in agreement with those available in the literature [3]. It is noteworthy that the coulombic efficiency of the electrode even after 100 cycles is 97%, which shows that the alloy performs well. The apparent activation energy ($\Delta_r H^*$) of the charge-transfer reaction occurring on the metal hydride electrode surface can be obtained from:

$$\log\left(\frac{T}{R_{ct}}\right) = -\frac{\Delta_r H^*}{2.3RT} + A \tag{5}$$

where A is a constant. In Fig. 7 $\log(T/R_{ct})$ is plotted against $1000/T$, from which the apparent activation energy at 100% state-of-charge is calculated as $49.01\,\mathrm{kJ\,mol^{-1}}$. This value is higher than that reported by Yuan and Xu [22]. The high value indicates high surface activity at the interface. On the other hand, the plot also shows that the catalytic activity of the negative electrode decreases with increase in temperature.

The main electrochemical reactions that occur at the metal hydride electrode are

$$M + H_2O + e^- \Leftrightarrow MH_{ads} + OH^{-1} \tag{6}$$

$$MH_{ads} \Leftrightarrow MH_{abs} \tag{7}$$

$$MH_{abs} \Leftrightarrow MH_{hyd} \tag{8}$$

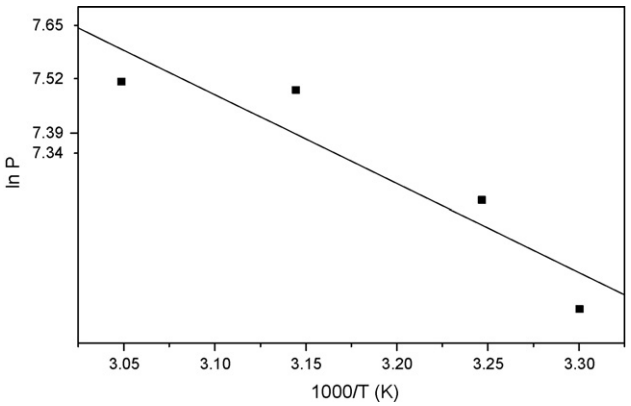

Fig. 6. van't Hoff plot for $MmNi_{3.03}Si_{0.85}Co_{0.60}Mn_{0.31}Al_{0.08}$ electrode.

where H_{ads}, H_{abs}, and H_{hyd} represent hydrogen adsorbed on the surface, absorbed on the surface, and in hydride form, respectively [23]. During charging, hydrogen is adsorbed on the electrode surface, which is subsequently absorbed into the bulk by diffusion and is converted into metal hydride according to Eqs. (6)–(8). Generally, the relative rate of individual reactions and especially the coulombic efficiency of hydrogen entry and withdrawal in metal hydride systems strongly depend on the magnitude of the metal–hydrogen interactive energy which, in turn, depends on temperature. The electro-reduction of water molecules becomes slower whereas the rate of hydrogen evolution increases. The hydrogen diffusion in a charge–discharge reaction is influenced by both the micro- and the macro-structure of the alloy. The diffusion coefficient of atomic hydrogen in the solid phase was shown to depend on the strength of the metal–hydrogen interaction and the hydrogen concentration in the bulk since this is a characteristic of mass transport in metal hydride electrodes [23]. The hydrogen diffusion coefficient (D) under galvanostatic discharge conditions was calculated as proposed by Zheng et al. [23]:

$$D = \frac{i_d r^2}{15(Q_0 - \tau i_d)} \tag{9}$$

where i_d = discharge current density ($\mathrm{A\,g^{-1}}$); r is average radius of the alloy particle (cm); Q_0 is the initial specific capacity ($\mathrm{C\,g^{-1}}$); τ is transient time (s), which is the time required for the sur-

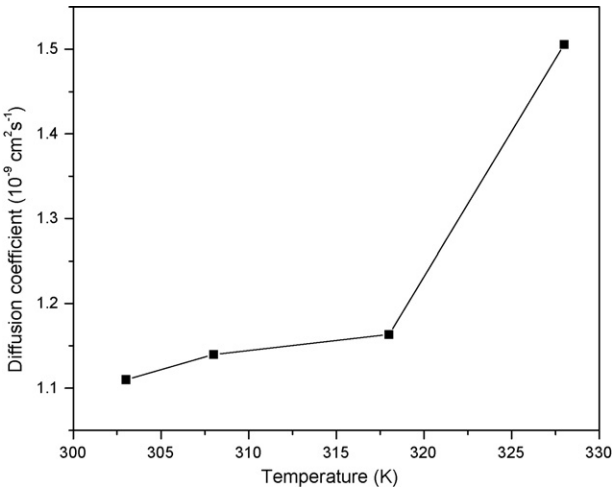

Fig. 8. Diffusion coefficient values at various temperatures for $MmNi_{3.03}Si_{0.85}Co_{0.60}Mn_{0.31}Al_{0.08}$ electrode.

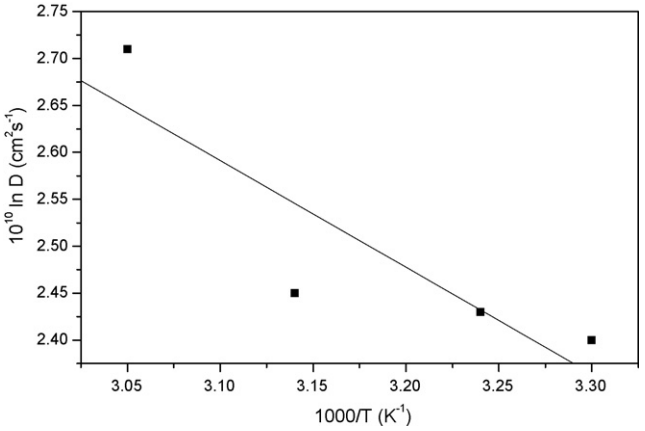

Fig. 9. Arrhenius relation for diffusion of hydrogen at various temperatures.

face concentration of hydrogen to become zero. It is clear from the data presented in Fig. 8 that the D values increase with increasing temperature, namely, 1.11×10^{-9} cm^2 s^{-1} at 303 K to 1.51×10^{-9} cm^2 s^{-1} at 328 K. This implies that hydrogen diffusion is faster at higher temperatures. The increase in the value of D may be ascribed to a lowering of the barrier for hydrogen diffusion due to easier dissolution of surface oxides at elevated temperatures [22]. An Arrhenius plot of D against temperature is shown in Fig. 9. The activation energy for hydrogen diffusion calculated from this plot is 23.60 kJ mol^{-1}, which is comparable with the results of Sequeira et al. [24].

Nyquist plots of fully charged metal hydride electrodes at various temperatures are given in Fig. 10. The plots consist of a small semicircle, a large semicircle and a straight line in the high-, medium- and low-frequency regions, respectively. The high-frequency arc and the middle-frequency arc are severely depressed

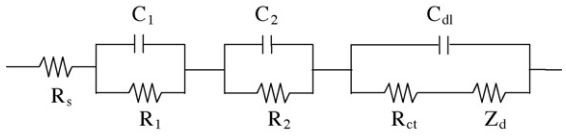

Fig. 11. Equivalent circuit for the Nyquist plot.

due to the porous nature of the alloy electrode. The impedance value at 328 K is drastically reduced. This indicates the formation of β-phase. The low-frequency arc represents the hydrogen evolution reaction. The Warburg impedance is due to the hydrogen absorption reaction. It is not explicitly exhibited in the present study since the frequency is limited to 5 mHz.

Raju et al. [25] recently explained capacity deterioration during various charge cycles based on impedance measurements. Impedance plots obtained at different temperatures at 100% state-of-charge were fitted by a non-linear least-squares fitting method with an equivalent circuit [26] (Fig. 11) to obtain the electrode kinetic parameters (Table 1). The intercept at high-frequency region is directly related to electrolyte resistance (R_s). The semicircle in the high-frequency region represents contact resistance (R_1) and contact capacitance (C_1) between the current collector and the active material. R_2 and C_2 represent the contact impedance between the alloy particles. R_{ct} denotes the charge-transfer resistance at the electrode-electrolyte interface. The double-layer capacitance, C_{dl}, is usually represented as Q_{cpe}, which is represented by a double-layer, constant-phase element on the electrode surface. Hydrogen diffusion behaviour is indicated as a straight line in the lower frequency region (Z_d). The absence of Warburg impedance in the impedance spectrum may be attributed to the porous nature of the electrode [26]. It can be seen from the plots that the total impedance decreases as the temperature is raised. The charge-transfer resis-

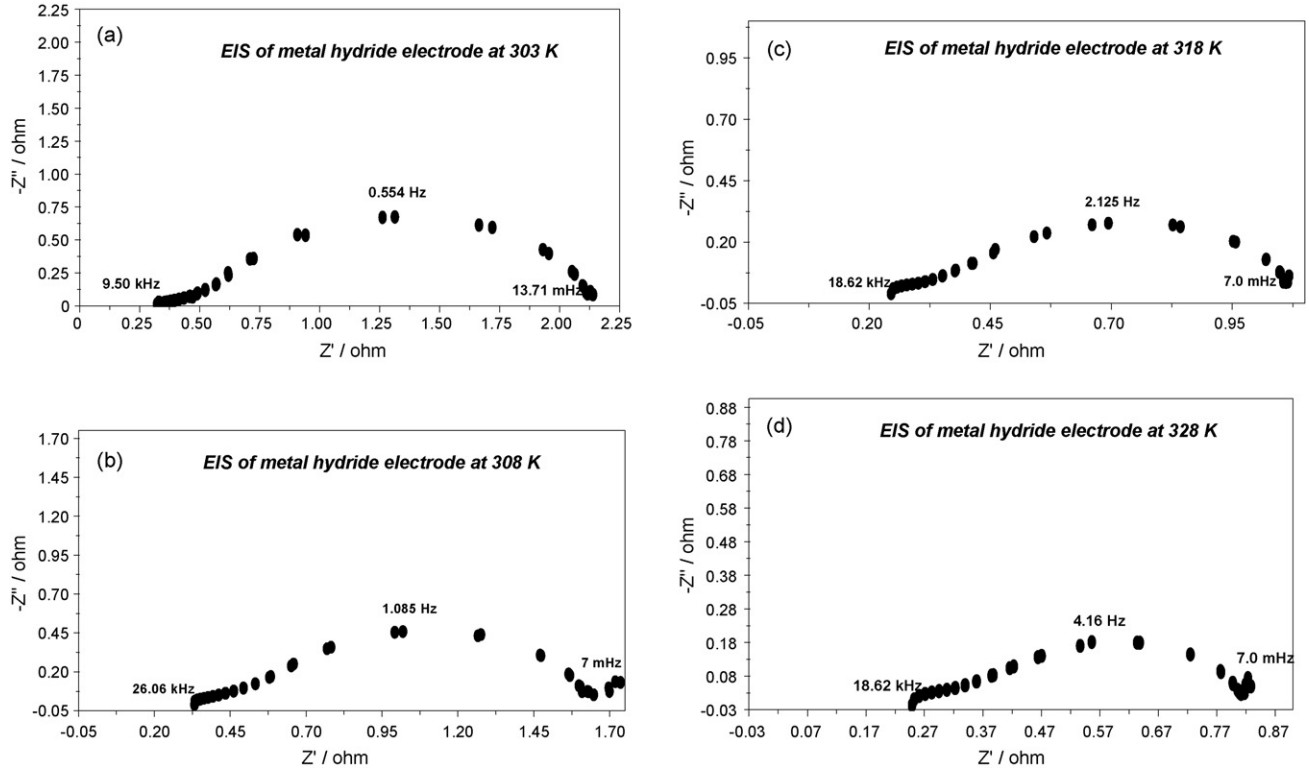

Fig. 10. (a–d) Nyquist plots for the $MmNi_{3.03}Si_{0.85}Co_{0.60}Mn_{0.31}Al_{0.08}$ electrode at various temperatures.

Table 1
Kinetic parameters of $MmNi_{3.03}Si_{0.85}Co_{0.60}Mn_{0.31}Al_{0.08}$ alloy electrode obtained by fitting the electrochemical impedance spectrum at different temperatures

Parameters	Temperature (K)			
	303	308	318	328
R_s ($\Omega\,cm^2$)	0.337	0.339	0.252	0.256
R_1 ($m\Omega\,cm^2$)	91.5	87.2	60.9	61.7
C_1 (mF)	1.054	1.237	1.050	0.983
R_2 ($m\Omega\,cm^2$	190.9	165.7	110.9	90.0
C_2 (mF)	22.46	16.88	14.69	12.24
R_{ct} ($\Omega\,cm^2$)	1.581	1.129	0.670	0.427
C_{dl} (mF)	113.7	84.7	66.3	63.9
Z_d	0.1074	0.1520	0.1688	0.2252

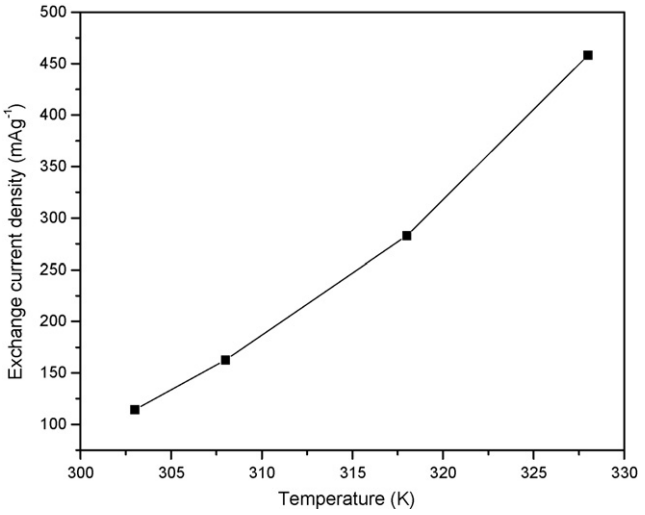

Fig. 12. Exchange current density of $MmNi_{3.03}Si_{0.85}Co_{0.60}Mn_{0.31}Al_{0.08}$ electrode at various temperatures.

tance decreases from 1.581 $\Omega\,cm^2$ at 303 K to 0.427 $\Omega\,cm^2$ at 328 K. This observation suggests that hydrogen evolution reaction proceeds more readily at higher temperatures, which may be due to the greater electrocatalytic activity of hydride-forming electrodes at higher temperatures.

Apart from thermodynamic properties, an important criterion for the selection of a metal hydride system is the kinetics of hydrogen electrosorption–desorption. This may be deduced from the value of the apparent exchange current density and polarization resistance, which are measures of the alloy's catalytic activity. The ohmic resistance, R_o is calculated by adding R_s, R_1 and R_2. R_{ct} and R_o decrease with increasing temperature. The decrease in R_{ct} implies a faster reaction rate at higher temperatures. This is reflected in the value of the exchange current density at different temperatures, as calculated by

$$i_o = \frac{RT}{nF}\left(\frac{1}{R_{ct}}\right) \quad (10)$$

where F is the Faraday constant. The exchange current densities vary between 114.23 $mA\,g^{-1}$ at 303 K and 458.00 $mA\,g^{-1}$ at 328 K (Fig. 12). The decrease of R_o may be explained by considering the conductivity of the electrolyte, which decreases with increasing temperature. It can be seen from Fig. 12 that the exchange current density increases with increasing temperature, which suggests that the electrode reaction becomes more reversible at higher temperatures. Both exchange current density and diffusivity increase with temperature, which implies that the discharge capacity and charge–discharge efficiency should increase with increasing temperature. At high temperatures, however, metallic phases become oxidized, which decreases the hydrogen evolution reaction, discharge capacity and the charge–discharge efficiency. Raising the temperature also increases the activation enthalpy of the charge-transfer reaction.

4. Conclusions

A lanthanum-rich metal hydride alloy $MmNi_{3.03}Si_{0.85}Co_{0.60}Mn_{0.31}Al_{0.08}$ has been prepared as a hydrogen storage electrode and its electrochemical hydrogen absorption/desorption characteristics have been investigated. Changes in enthalpy and entropy associated with the reactions are calculated as −41.74 $kJ\,mol^{-1}$ and 146.28 $J\,mol^{-1}\,K^{-1}$, respectively. It is found that the charge-transfer resistance decreases with increase in temperature. The exchange current density and diffusion coefficient are also shown to increase with temperature. It is concluded that capacity deterioration at elevated temperatures is associated with higher surface activity.

Acknowledgements

The authors thank the Director, CECRI for his encouragement and permission to publish this work. Thanks are also due to Dr. N.G. Renganathan of the Electrochemical Power Systems Division, CECRI and Dr. G. Balachandran of the Rare Earth Processing Group, DMRL, Hyderabad for useful discussions and for preparing the alloy, respectively.

References

[1] K. Hong, J. Power Sources 96 (2001) 85.
[2] A. Züttel, Naturwieeenschaften 91 (2004) 157.
[3] S. Bliznakov, E. Lefterova, L. Bozukov, A. Popov, P. Andreev, Proceedings of the International Workshop "Advanced Techniques for Energy Sources Investigation and Testing", September 4–9, Sofia, Bulgaria, 2004.
[4] C.S. Wang, X.H. Wang, Y.Q. Lei, C.P. Chen, Q.D. Wang, Int. J. Hydrogen Energy 22 (1997) 1117.
[5] J. Kleperis, F. Wojcik, A. Czerwinski, J. Skowronski, M. Kopczyk, M. Beltowska-Brzenska, J. Solid-State Electrochem. 5 (2001) 229.
[6] S.R. Ovshinsky, M.A. Fetcenko, J. Ross, Science 260 (1993) 176.
[7] K. Hong, US Patent 5,006,328 (1991).
[8] M.V.C. Sastri (Ed.), Metal Hydrides: Fundamentals and Applications, Narosa Publishing House, New Delhi, 1998.
[9] P.C.P. Bouten, A.R. Miedema, J. Less Common Met. 71 (1980) 147.
[10] H. Oesterreicher, Appl. Phys. 24 (1981) 169.
[11] R. Griessen, Phys. Rev. B 38 (1988) 3690.
[12] A. Shilov, M.E. Kost, N.T. Kuznetsov, J. Less Common Met. 128 (1987) 1.
[13] Z. Shuang, L. Qin, C. Ning, M. Li, Y. Wen, J. Alloy Compd. 287 (1999) 57.
[14] N. Mani, T.R. Kesaven, S. Ramaprabhu, J. Phys. Condens. Matter 14 (2002) 3939.
[15] N. Mani, R. Sivakumar, S. Ramaprabhu, J. Alloy Compd. 337 (2002) 148.
[16] N. Mani, S. Ramaprabhu, Int. J. Hydrogen Energy 30 (2005) 53.
[17] N. Mani, S. Ramaprabhu, J. Alloy Compd. 363 (2004) 275.
[18] M. Kandavel, S. Ramaprabhu, J. Phys. Condens. Matter 15 (2004) 7501.
[19] G. Zheng, B.N. Popov, R.E. White, J. Electrochem. Soc. 142 (1995) 2695.
[20] B.N. Popov, G. Zheng, R.E. White, J. Appl. Electrochem. 26 (1996) 603.
[21] X. Yuan, N. Xu, J. Alloy Compd. 316 (2001) 113.
[22] X. Yuan, N. Xu, J. Electrochem. Soc. 149 (2002) A407.
[23] G. Zheng, B.N. Popov, R.E. White, J. Electrochem. Soc. 143 (1996) 834.
[24] C.A.C. Sequeira, Y. Chen, D.M.F. Santos, J. Electrochem. Soc. 153 (2006) A1863.
[25] M. Raju, K. Manimaran, M.V. Ananth, N.G. Renganathan, Int. J. Hydrogen Energy 32 (2007) 1721.
[26] W. Zhang, M.P. Sridhar Kumar, S. Srinivasan, J. Electrochem. Soc. 142 (1995) 2935.